

Magnetic moment and anisotropy at the Fe/ZnSe(001) interface studied by conversion electron Mössbauer spectroscopy

F. Gustavsson,^{1,2,*} E. Nordström,¹ V. H. Etgens,³ M. Eddrief,³ E. Sjöstedt,¹ R. Wäppling,¹ and J.-M. George²

¹*Department of Physics, Uppsala University, Box 530, 75121 Uppsala, Sweden*

²*Unité Mixte de Physique CNRS-Thales, Domaine de Corbeville, 91404 Orsay, France*

³*LMCP, Université Paris VI-VII, 4 Place Jussieu, 75252, France*

(Received 20 February 2002; published 26 June 2002)

The interface magnetic properties of Fe/ZnSe heterostructures grown on GaAs(001) by molecular-beam epitaxy have been investigated using conversion electron Mössbauer spectroscopy (CEMS) and macroscopic magnetic measurements. For Fe films thinner than 100 Å an in-plane $\langle 110 \rangle$ uniaxial magnetic anisotropy was found and the magnetization loops could successfully be described by the simple Stoner-Wohlfarth model, which implies that the magnetization reverses only by coherent rotation and jump processes. For the interface analysis, a 5-Å-thick layer of enriched ^{57}Fe was deposited on the ZnSe surface and buried under 20 Å of natural Fe. In this way the ^{57}Fe serves as a local probe of the interface magnetic environment in a bulklike Fe film since the CEMS technique is only sensitive to this isotope of Fe. An interface magnetic moment of $2.18 \mu_B$ was found and, in relation to $2.2 \mu_B$ for bulk bcc Fe, this precludes the presence of any interface reactions. Surprisingly, however, the direction of the interface magnetic moment turned out to be reoriented from the $[110]$ direction by almost 30° , an effect that was assumed to arise from the distribution of unidirectional tetrahedral bonds present on the Zn $c(2 \times 2)$ reconstructed ZnSe surface.

DOI: 10.1103/PhysRevB.66.024405

PACS number(s): 75.70.Cn, 76.80.+y

INTRODUCTION

In the search for an integrated semiconductor spintronic device structure that efficiently exploits both the electron's spin as well as its charge, important progress has been reported recently.¹⁻³ Malajovich *et al.*³ demonstrated a coherent spin transfer with high efficiency through the GaAs/ZnSe semiconductor interface where circularly polarized light was used to excite spin-polarized carriers into the conduction band of GaAs. It has been pointed out though that before true success in semiconductor spintronics can be achieved, a stable source of spin-polarized carriers in which the spin alignment can be easily manipulated must be found.⁴ Optimally suited for this purpose would be the ferromagnetic transition metals, which exhibit intrinsic spin polarization even at elevated temperatures. When combined with semiconductors, however, most of these systems suffer from interface reactions resulting in severely suppressing effects on the spin transfer efficiency. As an example, a spin injection efficiency of 2% was observed⁵ in a GaAs/(In,Ga)As light-emitting diode covered with Fe and, although an encouraging result, the relatively low efficiency is most probably due to the formation of reacted phases with reduced magnetic moment commonly occurring at the Fe/GaAs interface.^{6,7}

Another characteristic feature of Fe(001) layers grown on a number of different semiconductors is the observed $\langle 110 \rangle$ in-plane uniaxial magnetic anisotropy (UMA),⁸⁻¹¹ which is at variance with the cubic symmetry of bulk bcc Fe. The origin of the UMA remains an open issue but has generally been suggested to derive from semiconductor attributes such as surface reconstructions and/or unidirectional bonds capable of distorting the cubic symmetry of the Fe layers.

In this work, the interface magnetic properties of Fe/ZnSe/GaAs(001) heterostructures grown by molecular-beam epitaxy (MBE) are investigated. From the device aspect, the Fe/ZnSe heterostructure is considered to be a promising can-

didate as spin aligner since the wide gap semiconductor ZnSe ($E_g = 2.7$ eV) could provide the interface resistance (or tunnel barrier) predicted to be essential in transferring spins from a transition metal into a degenerate semiconductor.¹² In an early work,¹³ the Fe/ZnSe interface was shown to be less reactive than, e.g., the Fe/GaAs interface and, recently,⁹ no loss of magnetic moment at the interface was claimed for Fe films grown on ZnSe at room temperature. In the latter case, however, the conclusion was made without demonstrating an interface specific investigation and, furthermore, on Fe films of inadequate quality for spintronic applications due to the low deposition temperature. In the present case, it will be shown that with conversion electron Mössbauer spectroscopy (CEMS), information about *both* magnetic moment and anisotropy can be obtained on a local scale. Since the technique is sensitive only to the ^{57}Fe isotope, selective regions, e.g., the interface, can be probed by incorporating ^{57}Fe layers exclusively at these regions. Additional magnetic characterization is performed with alternating gradient magnetometry (AGM).

EXPERIMENT

The samples were grown in a multichamber UHV system with separate III-V and II-VI MBE chambers and *in situ* techniques such as reflection high-energy electron diffraction (RHEED), x-ray photoemission spectroscopy (XPS), and scanning tunneling microscopy/spectroscopy (STM/STS). Details about the ZnSe substrate preparation are given elsewhere.¹⁴ In short, after deposition of a GaAs buffer layer on a GaAs(001) substrate, 100 Å of ZnSe is grown by atomic layer epitaxy. The surface is terminated Zn rich and stabilized to a Zn(2×2) reconstruction after annealing the sample to 350 °C.

For the CEMS measurements, two types of Fe films with enriched ^{57}Fe inclusion layers were prepared at a substrate

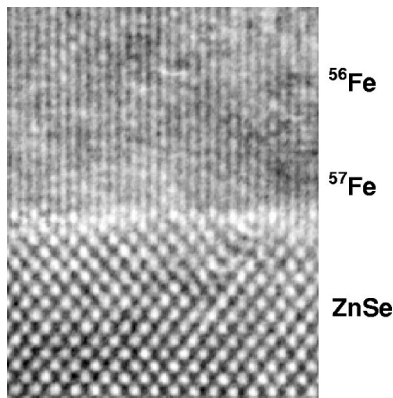


FIG. 1. TEM cross section of the Fe/ZnSe(001) interface.

temperature of 180 °C. The ^{57}Fe isotope enrichment in these layers amounts to 96%. In the first sample, denoted the interface sample, 5 Å (3.5 ML) of ^{57}Fe was deposited directly on the ZnSe epilayer followed by 20 Å of natural Fe. In this way, the interface properties of a bulklike Fe film can be probed, which is one of the outstanding advantages with the CEMS technique. The natural Fe only gives a small contribution ($\approx 7\%$) to the Mössbauer resonance intensity, due to the 2% ^{57}Fe content, and would show up as mainly a bulk contribution. In the second sample, a 5-Å ^{57}Fe layer was sandwiched between 10 Å of natural Fe to serve as a bulklike reference for the spectral analysis of the interface sample. A capping layer of 5 Å Au was used for both samples. Film thicknesses were calibrated by means of XPS and transmission electron microscopy (TEM).

Recent XPS and STM/STS experiments¹⁵ have shown that Fe forms a continuous film above one monolayer at this growth temperature and proceeds in a two-dimensional fashion, which confirms the previous work of Jonker and Prinz.¹³ In order to study the interface morphology in more detail, a sample was prepared for TEM. Figure 1 shows a TEM cross section of the Fe/ZnSe interface and, apart from excellent heteroepitaxy, the interface appears abrupt with no visual evidence of intermixing.

The CEMS measurements were performed in a vacuum system ($p < 10^{-6}$ mbars) in which samples can be cooled down to 4 K using a continuous He flow cryostat. The γ ray emitted from a radioactive source enters the vacuum chamber through a thin Al window and, in contrast to the more conventional case of normal incidence, the γ ray has an incident angle of 45° to the sample normal. In this geometry, the plane projected component of the γ ray allows determination of the in-plane direction of magnetization, an information that is not accessible at normal incidence. The spectra were recorded with the γ ray projected along both the Fe[110] and Fe[1 $\bar{1}$ 0] crystallographic directions. The conversion electrons were detected using a channel electron multiplier and the velocity scale was calibrated using a spectrum from α -Fe recorded simultaneously. For the analysis of the spectra, the commercial software Recoil was employed. More details about the CEMS technique can be found in Ref. 16.

Complementary to the CEMS measurements, macro-

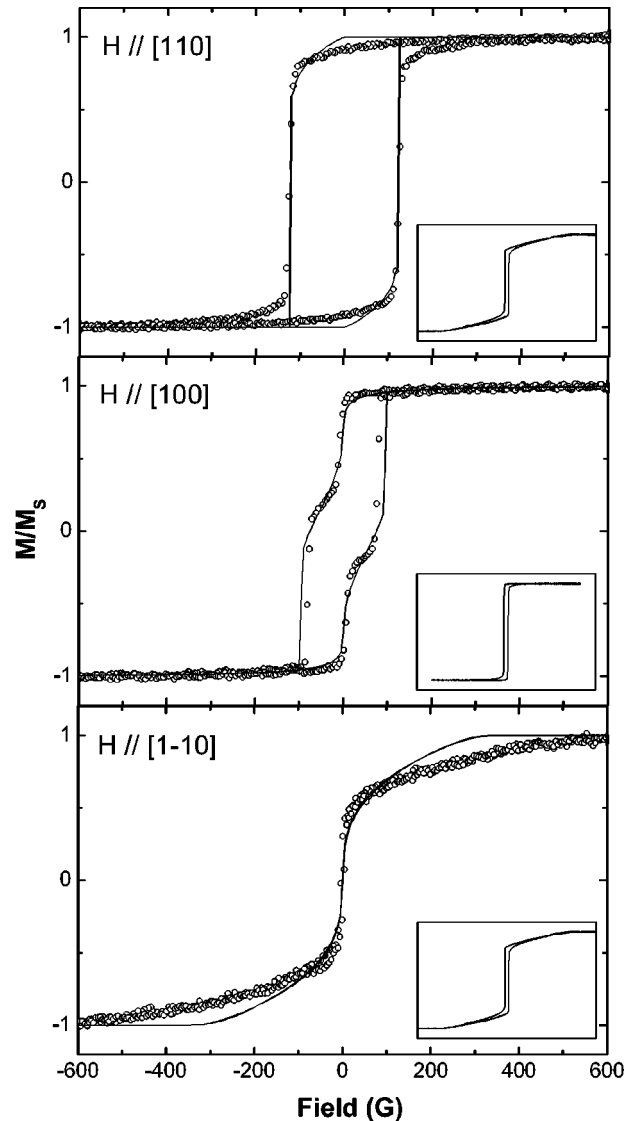


FIG. 2. AGM loops for a 25-Å Fe film on ZnSe(001) measured along three high-symmetry in-plane directions (open circles). A uniaxial magnetic anisotropy is found in the $\langle 110 \rangle$ directions with the easy axis oriented [110]. Solid lines represent fitted loops using the Stoner-Wohlfarth model (Ref. 17). The measured loops are reproduced with a ratio between the effective cubic and uniaxial anisotropy constants $K_1^{eff}/K_u^{eff} \approx 1$. Inset are magnetization curves for a 100-Å Fe film showing a recovery to cubic anisotropy with $\langle 100 \rangle$ equivalent easy directions.

scopic magnetic profiling was made with AGM for several in-plane orientations.

RESULTS AND DISCUSSION

AGM magnetization loops measured at room temperature along [110], [100], and [1 $\bar{1}$ 0] in-plane directions of a 25-Å-thick Fe film on ZnSe are shown in Fig. 2 (open circles). Seemingly, the Fe film displays a uniaxial anisotropy character similar to that found in Refs. 8–11. The [1 $\bar{1}$ 0] direction represents a magnetically hard axis with virtually zero remanence and coercivity. In the [110] direction, the highly

coercive square-type loop indicates an easy axis. Along [100], which is the expected easy direction for a monocrystalline bulk bcc Fe film, two distinct switching fields are observed. At first, this two-step reversal seems somewhat unexpected in an epitaxial single layer of Fe but, as will be shown, the system follows ideally the Stoner-Wohlfarth (SW) model of coherent rotation¹⁷ with mixed uniaxial and fourfold anisotropies.

Assuming a hard axis along the $[1\bar{1}0]$ direction, the total energy density of the film can be written as

$$E = K_u^{eff} \cos^2 \theta + \frac{K_1^{eff}}{4} \sin^2 2(\theta + \pi/4) - HM_s \cos(\theta - \phi), \quad (1)$$

where K_u^{eff} and K_1^{eff} are the effective uniaxial and cubic in-plane anisotropy constants, θ the angle between the spin orientation M and $[1\bar{1}0]$ and ϕ the angle between the applied field H and $[1\bar{1}0]$. By minimizing Eq. (1) with respect to θ ($dE/d\theta=0$ and $d^2E/d\theta^2>0$), a model magnetization loop can be obtained as $M_{mod} = \cos[\theta(H) - \phi]$. Subsequently, the experimental magnetization can be modeled by refining the K_u^{eff} and K_1^{eff} parameters until optimal agreement is reached. This is what has been done in Fig. 2, where the model magnetization loops are plotted as solid lines. Best agreement with the experimental curves results from an anisotropy ratio $K_1^{eff}/K_u^{eff}=0.97$, where $K_1^{eff}=1.25 \times 10^5$ erg/cm³ and $K_u^{eff}=1.29 \times 10^5$ erg/cm³ using $M_s = 1710$ emu/cm³ for Fe. As can be seen, the two switching fields in the [100] loop are well described by the model as well as the large coercivity in the [110] loop. In the $[1\bar{1}0]$ loop, a larger discrepancy is observed. The main reason for discrepancies comes from the sample alignment with respect to the applied field ($\Delta\phi \approx \pm 3^\circ$), which becomes most crucial in the hard direction. Also, thermal effects have a suppressing influence on the magnetization at low fields. For Fe films above 100 Å, the cubic anisotropy is recovered with $\langle 100 \rangle$ easy axes as shown in the insets in Fig. 2.

The effective anisotropies K_1^{eff} and K_u^{eff} are thickness dependent and can be divided into a volume term and an interface term as

$$K_{1(u)}^{eff} = K_{1(u)}^{vol} + \frac{K_{1(u)}^{Fe/ZnSe} + K_{1(u)}^{Au/Fe}}{t}, \quad (2)$$

where $K_{1(u)}^{Fe/ZnSe}$ and $K_{1(u)}^{Au/Fe}$ denote anisotropy contributions from the Fe/ZnSe and Au/Fe interfaces, respectively, and t is the Fe film thickness (25 Å in this case). Letting the cubic volume term to be analogous to the fourfold anisotropy coefficient of bulk Fe, i.e., $K_1^{vol} = 4.5 \times 10^5$ erg/cm³, and using $K_{1(u)}^{Au/Fe} = -2.5 \times 10^{-2}$ erg/cm² from Ref. 18, this yields $K_{1(u)}^{Fe/ZnSe} = -5.6 \times 10^{-2}$ erg/cm². In the uniaxial case, K_u^{vol} can be put to zero as the uniaxial anisotropy is of pure interface character and using $K_u^{Au/Fe} = 0$ (Ref. 18), this gives $K_u^{Fe/ZnSe} = 3.2 \times 10^{-2}$ erg/cm². Comparing the $K_{1(u)}^{Fe/ZnSe}$ and $K_u^{Fe/ZnSe}$ values with the ones found in Ref. 9, it turns out that $K_{1(u)}^{Fe/ZnSe}$ is a factor two larger whereas $K_u^{Fe/ZnSe}$ is about half the corresponding values in the reference. It is believed that

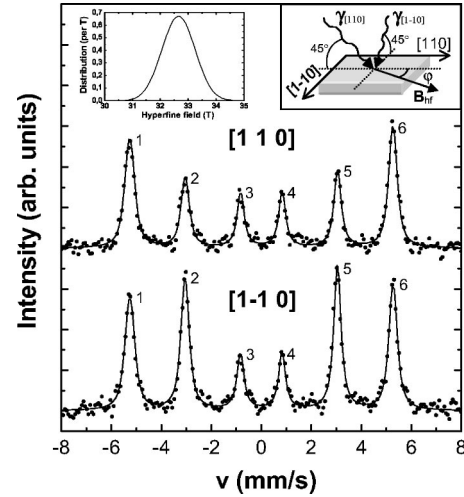


FIG. 3. Room-temperature CEMS spectra of a Fe(20 Å)/⁵⁷Fe(5 Å)/ZnSe(001) sample with the plane-projected γ ray along Fe[110] (top spectrum) and Fe[$1\bar{1}0$] (bottom spectrum). Solid lines represent a one-site model fit (see text). The left inset shows the distribution of the hyperfine field resulting from the one-site model and the right inset illustrates the experimental geometry.

the improved crystalline quality of the Fe films when grown at 180 °C compared to RT in Ref. 9 is responsible for the discrepancies.

The fact that the switching fields can be reproduced quantitatively by the simple SW model suggest that the Fe film is practically free from defects and of ideal single domain type. Defects inducing, e.g., domain-wall pinning sites would cause switching fields different from the ones predicted by the SW model. In a single domain sample, the magnetization reverses by rotation and either one or two irreversible jumps. These jumps occur at distinct switching fields that depend exclusively on the anisotropy ratio K_1/K_u and the applied field orientation, which is clearly the case for this sample. Jump processes have been studied in detail in Ref. 19.

Anisotropic lattice relaxation has previously been suggested to be responsible for the UMA in Fe/semiconductor structures.¹⁰ In order to investigate these effects, RHEED measurements were performed along both Fe[110] and Fe[$1\bar{1}0$] directions. Even though an anisotropic lattice relaxation was detected for low coverage, it disappeared above 15 Å as the bulk lattice parameter of Fe was gradually approached in a similar way for both directions. Since it is reasonable to believe that the anisotropic history is erased by the relaxation to the bulk lattice, magnetoelastic effects are not likely to induce the UMA of the 25-Å Fe film studied here.

In Fig. 3, room-temperature CEMS spectra of the Fe(20 Å)/⁵⁷Fe(5 Å)/ZnSe interface sample recorded along Fe[110] and Fe[$1\bar{1}0$] are shown. The clean sextets reveal a distinct hyperfine magnetic-field splitting without traces of atomic sites with reduced field. The intensity variations between the [110] and the $[1\bar{1}0]$ spectrum are directly related to the direction of the hyperfine field as will be discussed further below. First, in order to extract some Mössbauer pa-

rameters, a single-site model is used in which it is assumed from the well-defined sextets that all ^{57}Fe sites are equivalent but with a distribution in hyperfine field. A simulation of the spectra converges to an average hyperfine field of 32.7(2) T with a 0.65-T distribution as shown in the inset in Fig. 3. The field is in good agreement with the bulk value of 33.0 T for bcc Fe, which implies that no chemical reactions have occurred at the interface. This result is also in accordance with recent x-ray magnetic circular dichroism measurements on ultrathin Fe layers on ZnSe.¹⁵ Expressed in Bohr magnetons, using the conversion factor of 15 T/ μ_B , a hyperfine field of 32.7 T corresponds to a magnetic moment of 2.18 μ_B . The isomer and the quadrupole shifts obtained from the model are very small, both around 0.003 mm/s compared to α -Fe. This suggests that the vast majority of the ^{57}Fe sites sense a bcc Fe-type surrounding. Similar results are obtained at 30 K but with an increase in hyperfine field of about 4%.

The relative intensities in a Mössbauer spectrum in the case of a pure magnetic interaction are related to the angle α between the incident γ ray and the magnetization by

$$I_{1,6} = 3(1 + \cos^2 \alpha), \quad I_{2,5} = 4 \sin^2 \alpha, \quad I_{3,4} = 1 + \cos^2 \alpha, \quad (3)$$

as derived from the angle-dependent Clebsch-Gordan coefficients that describe the different transition probabilities. Expressed as intensity ratios, this gives

$$I_{1,6} : I_{2,5} : I_{3,4} = 3 : 4 \sin^2 \alpha / (1 + \cos^2 \alpha) : 1. \quad (4)$$

A quantitative measure of α can then be deduced from the intensity ratio between peaks 2,5 and 3,4 in Eq. (4) by the relation $\alpha = \arcsin \sqrt{2/(1 + 4/I_{2,5})}$. Keeping in mind that the incident γ ray is 45° to the sample plane, the in-plane angle φ between the plane-projected γ ray and the hyperfine field (see right inset in Fig. 3) can be obtained through the relation $\cos \varphi = \sqrt{2} \cos \alpha$. Now, looking at the intensity relations between the [110] spectrum and the $[1\bar{1}0]$ spectrum in Fig. 3, it is evident that the intensities of the second and fifth peak are suppressed considerably in the [110] case compared to $[1\bar{1}0]$. From the model spectra, the $I_{2,5}$ ratios are found to be 1.70(7) for [110] and 3.10(11) for $[1\bar{1}0]$, which correspond to in-plane angles of $\varphi = 26(3)^\circ$ and $\varphi = 60(3)^\circ$ relative to these directions, respectively. The major contribution to the discrepancy between these values is the accuracy of the sample alignment that is estimated to be $\pm 3^\circ$. Thus, on average, the magnetic moment of the 3.5 ML ^{57}Fe at the interface is oriented almost 30° from [110] and indeed this is an unexpected result.

Identical spectral features were obtained after the interface sample had been exposed to an applied field of 0.6 T along [110] in order to force alignment of the magnetic domains, which rules out a distribution of magnetic domain orientations also supported by the AGM measurements. However, on the reference sample of equal Fe thickness (25 Å) but with 3.5 ML ^{57}Fe confined in the center as a bulk probe, the magnetic moment was found to be oriented along [110]. This was also the direction along which the highest remanence was found in the magnetic measurements. There-

fore, if the interface and the reference sample can be considered identical, it appears that the magnetic moment near the interface is reoriented.

Focusing again on the analysis of the interface sample, it is reasonable to believe that the ^{57}Fe atoms in the 5-Å-thick interface layer occupy at least two types of sites, one of interface character and the other one bulk. A closer inspection of the spectra in Fig. 3 reveals that the peaks on the positive side are somewhat higher in intensity and more narrow than the corresponding peaks on the negative side. Therefore, it is not excluded that the peak asymmetry reflects contributions from two (or more) sites with slight differences in Mössbauer shifts. In the single-site model used above, the asymmetry was compensated for by allowing a distribution of the isomer shift in connection with the field distribution. This had a negligible effect on quantities of interest and was merely introduced to reproduce the spectra more closely. Considering now a two-site contribution, the unexpected off-symmetry direction of the hyperfine field could then, in principle, result from a superposition of two similar components with hyperfine fields in different high-symmetry directions. It was found that, on attempting a two-site model, the spectra could indeed be reproduced with one site oriented [110] as the bulk reference and the other site, thus representing the interface, oriented either [100] or $[1\bar{1}0]$. The resulting bulk/interface site populations were 51%/49% and 74%/26% for the [110]/[100] and [110]/ $[1\bar{1}0]$ cases, respectively. It is worth mentioning here that a separation into two contributing sites is, in the present case, neither straightforward nor reliable since the recorded spectra very closely resemble that of the α -Fe reference but with some line broadening. It is well known that when modeling a spectrum with two or more components in such a situation, the resulting parameter values are of ambiguous character.

Exactly what might cause the 30° rotation from [110] of the interface magnetic moment is not evident. Since it was shown that the bulk value of the magnetic moment subsists at the interface, a formation of FeZn or FeSe reacted phases can be ruled out as to be responsible for the reorientation since these phases would reduce the magnetic moment most definitely and show up as separate components in the Mössbauer spectra. A recent electronic structure calculation predicts that the unidirectional nature of the surface bonds on unreconstructed ZnSe surfaces can be held responsible for the in-plane UMA of the Fe overlayers.²⁰ Each surface atom has two unsatisfied tetrahedral bonds and depending on whether the surface is terminated Zn or Se rich, they are oriented along $[1\bar{1}0]$ or [110]. In the calculation it was found that the orientation of the easy axis preferred to be orthogonal to the tetrahedral bonds. Experimentally, however, a clean fcc ZnSe surface is difficult to achieve since it is not stable in the temperature window where continuous epitaxial films are formed and the result is a reconstructed surface. Different types of reconstructions can in most cases be obtained by thermal annealing. In the present case, the ZnSe surface has been stabilized to a $c(2 \times 2)$ Zn rich reconstruction, which describes a half covered surface of undimerized Zn atoms.²¹ Due to the sparseness of this surface, un-

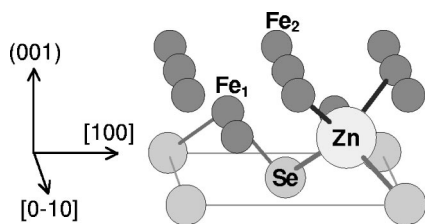


FIG. 4. Interface cell of Fe/ZnSe:Zn $c(2 \times 2)$ assuming ideal stacking positions. The first 3/4 ML Fe goes in the same plane as the half covered Zn surface satisfying the $[110]$ unidirectional Se subsurface bonds while the second full ML Fe satisfies the $[1\bar{1}0]$ unidirectional Zn surface bonds.

satisfied bonds from the Se subsurface layer are left exposed. This means that the surface can no longer be regarded as to be of unidirectional character exclusively, but rather to consist of an equal distribution of $[1\bar{1}0]$ (Zn) and $[110]$ (Se) oriented bonds that are offset by one atomic layer.

Considering now the case when, for example, 2 ML of Fe is deposited. Assuming ideal stacking positions, a plausible arrangement of the Fe atoms is illustrated in Fig. 4. The first Fe layer levels with the Zn surface resulting in a coverage of 3/4 ML with one Fe-Se bond/interface cell. The second Fe layer reaches full coverage with one Fe-Zn bond/interface cell. Simply put, following the arguments in Ref. 20, the magnetic moment of the first layer strives to align with the $[1\bar{1}0]$ direction while the magnetic moment of the second layer strives for $[110]$. Thus, the resulting direction of the first 2 ML could be oriented in a direction in between $[1\bar{1}0]$ and $[110]$ as a result of an interplay between the magnetic anisotropy energies connected to each type of bond, Fe-Se or Fe-Zn. Qualitatively, this scenario could explain the observed reorientation of the interface magnetic moment. Nev-

ertheless, electronic structure calculations involving reconstructed surfaces are needed in order to quantify this result.

CONCLUSION

High quality Fe/ZnSe(001) heterostructures have been grown on GaAs(001) substrates by MBE. An in-plane uniaxial magnetic anisotropy for films thinner than 100 Å was confirmed by magnetization measurements. The magnetization loops could successfully be described by the simple Stoner-Wohlfarth model, with a uniaxial to cubic anisotropy constant ratio of nearly 1 for a 25-Å-thick Fe film, which evidences that the magnetization reverses solely by coherent rotation. By confining thin ^{57}Fe layers at selective positions in Fe/ZnSe(001) heterostructures, it was shown that local information about both magnetic moment and anisotropy can be extracted using conversion electron Mössbauer spectroscopy in a flexible geometry. An interface magnetic moment of $2.18 \mu_B$ was found at room temperature that is in good agreement with the bulk value of $2.2 \mu_B$ for bcc Fe. This precludes presence of interface reactions and, therefore, places the Fe/ZnSe bilayer as one of the top metal/semiconductor candidates for future spintronics applications. An unexpected reorientation of about 30° from the $[110]$ direction was found for the magnetic moment at the interface and was explained in terms of an equal distribution of unidirectional tetrahedral bonds present on the Zn $c(2 \times 2)$ reconstructed ZnSe surface.

ACKNOWLEDGMENTS

The Swedish Foundation of Strategic Research (SSF) and the Swedish Research Council (VR) are acknowledged for their support and F.G. acknowledges support from the French M.A.E.

*Email address: Fredrik.Gustavsson@fysik.uu.se

¹Y. Ohno, D. K. Young, B. Beschoten, F. Matsukura, H. Ohno, and D. D. Awschalom, *Nature (London)* **402**, 790 (1999).

²R. Fiederling, M. Keim, G. Reuscher, W. Ossau, G. Schmidt, A. Waag, and L. W. Molenkamp, *Nature (London)* **402**, 787 (1999).

³I. Malajovich, J. J. Berry, N. Samarth, and D. D. Awschalom, *Nature (London)* **411**, 770 (2001).

⁴M. L. Roukes, *Nature (London)* **411**, 747 (2001).

⁵H. J. Zhu, M. Ramsteiner, H. Kostial, M. Wassermeier, H.-P. Schnherr, and K. H. Ploog, *Phys. Rev. Lett.* **87**, 016601 (2001).

⁶A. Filipe and A. Schuhl, *J. Appl. Phys.* **81**, 4359 (1997).

⁷C. Lallaizon, B. Lépine, S. Ababou, A. Schussler, A. Quémerais, A. Guivarch, G. Jézéquel, S. Députier, and R. Guérin, *Appl. Surf. Sci.* **123/124**, 319 (1998).

⁸E. M. Kneedler, B. T. Jonker, P. M. Thibado, R. J. Wagner, B. V. Shanabrook, and L. J. Whitman, *Phys. Rev. B* **56**, 8163 (1997).

⁹E. Reiger, E. Reinwald, G. Garreau, M. Ernst, M. Zölf, F. Bensch, S. Bauer, H. Preis, and G. Bayreuther, *J. Appl. Phys.* **87**, 5923 (2000).

¹⁰Y. B. Xu, D. J. Freeland, M. Tselepi, and J. A. C. Bland, *Phys. Rev. B* **62**, 1167 (2000).

¹¹P. Ma and P. R. Norton, *Phys. Rev. B* **56**, 9881 (1997).

¹²A. Fert and H. Jaffres, *Phys. Rev. B* **64**, 184420 (2001).

¹³B. T. Jonker and G. A. Prinz, *J. Appl. Phys.* **69**, 2938 (1991).

¹⁴L. Carbonell, V. H. Etgens, A. Kobel, M. Eddrief, and B. Capelle, *J. Cryst. Growth* **201/202**, 502 (1999).

¹⁵M. Marangolo, F. Gustavsson, M. Eddrief, P. Saintavit, V. Etgens, V. Cros, F. Petroff, J. George, P. Bencok, and N. Brookes, *Phys. Rev. Lett.* **88**, 217202 (2002).

¹⁶*Ultrathin Magnetic Structures*, edited by B. Heinrich and J. A. C. Bland (Springer-Verlag Berlin, Heidelberg, 1994), Vol. II.

¹⁷E. C. Stoner and E. P. Wohlfarth, *Philos. Trans. R. Soc. London, Ser. A* **240**, 599 (1948).

¹⁸M. Brockmann, S. Miethaner, R. Onderka, M. Köhler, F. Himmelhuber, F. Bensch, T. Schweinböck, and G. Bayreuther, *J. Appl. Phys.* **81**, 5047 (1997).

¹⁹C. Daboo, R. J. Hicken, E. Gu, M. Gester, S. J. Gray, D. E. P. Eley, E. Ahmad, J. A. C. Bland, R. Ploessl, and J. N. Chapman, *Phys. Rev. B* **51**, 15 964 (1995).

²⁰E. Sjöstedt, L. Nordström, F. Gustavsson, and O. Eriksson (unpublished).

²¹S. Tomiya, R. Minatoya, H. Tzukamoto, S. Itoh, K. Itoh, K. Nakano, E. Morita, and A. Ishibashi, *J. Appl. Phys.* **82**, 2938 (1997).